

RECENT STUDIES OF THE ELECTRON CLOUD INDUCED BEAM INSTABILITY AT THE LOS ALAMOS PSR*

R. Macek[#], L. Rybarcyk, R. McCrady and T. Zaugg,
 LANL, Los Alamos, NM 87545, USA
 J. Holmes, ORNL, Oak Ridge, TN 37831, USA

Abstract

Recent beam studies have demonstrated that a stable beam with the standard production bunch width of 290 ns and near the e-p instability threshold will become unstable when the bunch width is shortened significantly. This was not the case years earlier when the ring rf operated at the 72.000 integer subharmonic of the Linac bunch frequency. The present operating frequency is set at the 72.070 non-integer subharmonic and appears to be responsible for the recently observed “short pulse instability phenomenon”. Experimental characteristics of the short pulse instability are presented along with comparisons to the instability under 72.000 subharmonic operating conditions.

INTRODUCTION

The electron cloud (EC) induced instability, also known as the two-stream e-p instability, has been observed ever since the PSR was commissioned in 1986 [1] and has been extensively studied since then. All the available evidence points to a two-stream instability from coupled motion of the proton beam and a “cloud” of low energy electrons. In our present picture of this instability, primary electrons arising mostly from beam losses are amplified by multipactor on the ~140 ns long trailing edge of the ~290 ns long beam pulse. Sufficient electrons survive the ~70 ns gap between bunch passages to be captured by the next bunch passage to drive the instability. The largest uncertainty in locating the main EC source is the distribution of primary electrons born at the chamber walls from grazing angle beam losses.

For the discussion to follow, it is helpful to understand the process for and signature of the instability threshold shown in Figure 1. During beam instability studies, we store a stable beam for typically 400 μs after the end of accumulation in order to allow the instability to develop at fixed beam intensity and in the absence of losses from H⁰ excited states which field strip part way into the first dipole downstream of the injection stripper foil. The ring rf buncher voltage is lowered until a) exponentially growing coherent motion is seen on a beam position monitor (BPM) in the ring and b) a significant beam loss shows on the sum signal from 19 loss monitors and ~5% loss of beam current appears by the time the beam is extracted. Thresholds obtained by the above criteria are reproducible to ~5% of the buncher voltage. For buncher voltages ~5% above the threshold the beam is stable. At lower buncher voltages, the instability is more

pronounced in that the losses are typically higher and the coherent motion and losses start earlier and may saturate.

The plot of instability threshold voltage as a function of beam intensity while all other beam parameters are held fixed is designated an **instability threshold curve**. These are typically linear in intensity (Q = charge stored/pulse) and have long been studied as a function of many beam setup parameters (e.g. emittance, bunch width, tune, multipole settings, buncher phase, etc) [2]. For instability threshold curves, the intensity is varied by beam jaws at the linac front end or by periodically chopping out a turn of injection. An example of threshold curves for 3 beam bunch lengths (PW, pattern width of one injected turn or mini-pulse) is shown in Figure 2 for data collected in 2001 when the PSR rf routinely operated at the exact 72.000 subharmonic of the linac frequency.

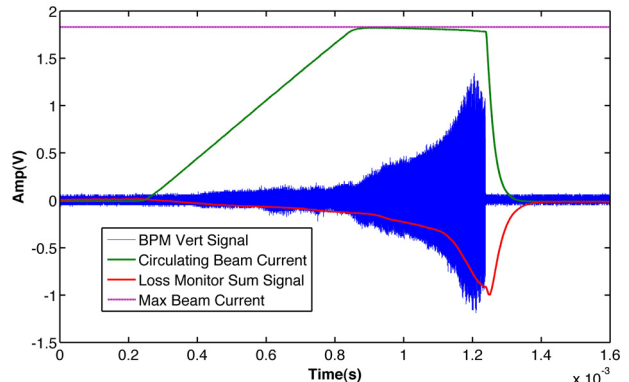


Figure 1: Experimental signature for the e-p threshold.

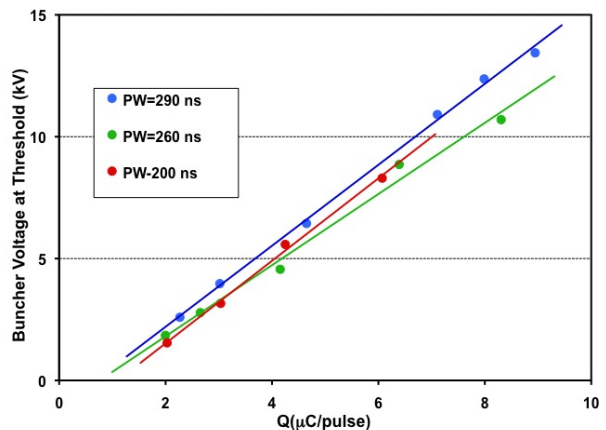


Figure 2: Instability threshold curves for various PW collected 5/26/2001 (72.000 subharmonic operation). Beam was accumulated for 1225 μs and stored for 400 μs after end of injection.

*This work was supported by the U. S. Department of Energy under contract DE-AC52-06NA25396.

[#]macek@lanl.gov

In Figure 2, the threshold curves show a typical linear behavior as a function of intensity with essentially the same curve for each PW such that the threshold curve depended only on stored charge/pulse and not the bunch width. Note that changing the PW does reduce the charge/macro-pulse (same as charge/turn) in these measurements where the accumulation time and store time after the end of accumulation is fixed along with the beam injection offset, which sets the beam size except for effects from space charge emittance growth. The very weak dependence on PW shown in Figure 2 persisted for several years until a major change in behavior was observed recently and is described in the next section.

It should be noted that the dependence on PW in Figure 2 is at considerable variance with the linear stability theory developed by Blaskiewicz et al in ref [3]. In this model the threshold charge depends linearly on the rf voltage and as the third power of bunch length. The bunch-width scaling for the new results discussed below for the non-integer subharmonic (72.070) conditions are found to be considerably more consistent with this model.

RECENT OBSERVATIONS OF EC INSTABILITY FOR SHORT PULSES

In 2009 it was observed that reducing the PW required more buncher voltage to keep the beam stable, which is in striking contrast to the behavior in earlier years. This phenomenon has been studied several times since then and was found to be reproducible for the present ring-operating regime (72.070 subharmonic of the linac bunch frequency). Examples of instability threshold curves for this regime are shown in Figure 3 and should be compared with those in Figure 2 that cover the same range of PWs and storage time (400 μ s). The comparison shows that the beams with shorter PW are now significantly less stable i.e., have an instability threshold voltage that is significantly higher for the same stored charge.

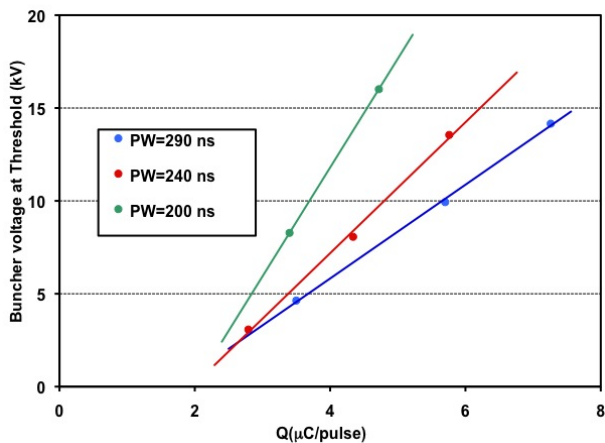


Figure 3: Instability threshold curves for various PW collected 9/25/2010 (72.070 subharmonic operation). Beam was accumulated for 825 μ s and stored for 400 μ s after end of accumulation.

Another set of threshold curves, covering a wider range of bunch widths (PW), is shown in Figure 4 and was collected with a shorter store time of 200 μ s that enabled us to go to even shorter PW without exceeding the maximum voltage on the rf buncher (~17 kV). The threshold curves in Figures 3 and 4 show that beams with shorter PW are progressively less stable as the PW is lowered. Also note that the curve for PW=290 in Figure 4 is somewhat lower than the corresponding curve in Figure 3. This is a typical behavior in that a longer store time requires a slightly higher rf buncher voltage to avoid instability, presumably because the instability has more time to develop after the end of accumulation.

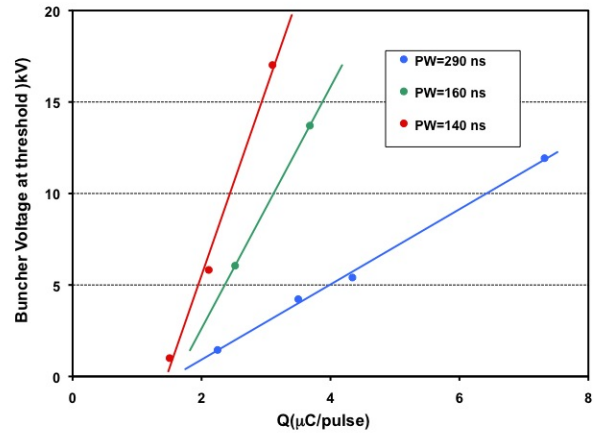


Figure 4: Instability threshold curves for various PW collected 9/24/2010 (72.070 subharmonic). Beam was accumulated for 825 μ s and stored for 200 μ s after end of accumulation.

The slopes of the instability threshold curves in Figure 3 and 4 are plotted as a function of PW in Figure 5. Fits to the data points using the $(PW)^{-3}$ law predicted in the model of ref [3] are shown. It should be noted that other values of the PW exponent from -2.5 to -4 fit reasonably well. The main point is the strong variation of the instability threshold curves with PW for 72.070 subharmonic operation compared with the no variation for 72.000 integer subharmonic operation of earlier years.

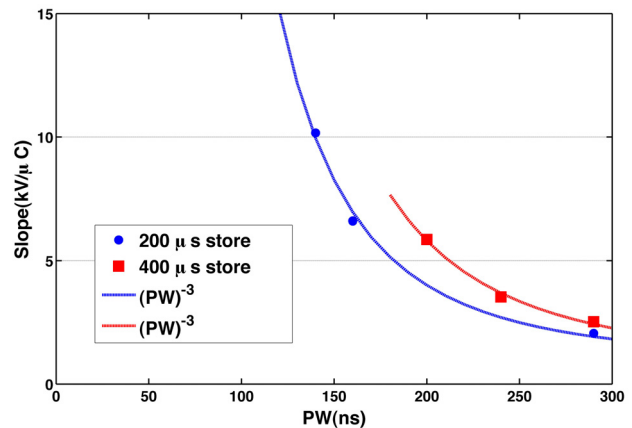


Figure 5: Slopes of the instability threshold curves of Figures 3 (red points) and 4 (blue points) plotted as a

function of PW. The continuous curves are fits [(PW)⁻³ plus a constant] to the respective data sets.

At the start of the 2010 LANSCE/PSR operating cycle the ring was inadvertently set to the 72.009 subharmonic of the linac frequency. This error was discovered when we investigated why the longitudinal beam profile showed more “hash” i.e. high frequency structure. This investigation (7/15/10) also revealed that lowering the PW for a 290 ns beam near threshold no longer made the beam unstable, which was the behavior observed for years when operating the ring at the 72.000 integer subharmonic. The ring was then set up for the 72.070 subharmonic in order to make a contemporaneous comparison with the 72.009 subharmonic data. The main results of this investigation are plotted in Figures 6 and 7 and discussed below.

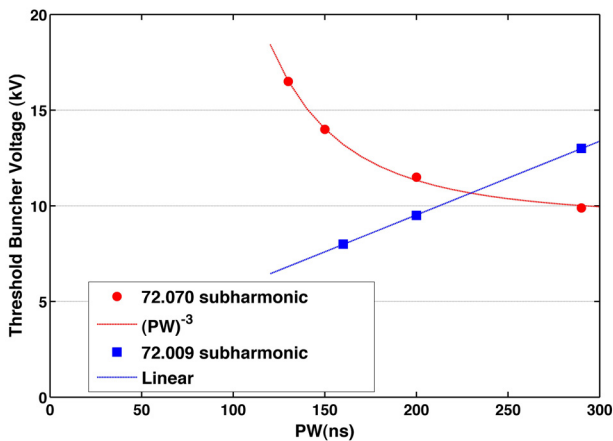


Figure 6: Comparison of instability threshold data plotted as a function of PW for ring operation at the 72.009 and 72.070 subharmonic of the linac bunch frequency. Also shown is a (PW)⁻³ fit to the 72.070 subharmonic data and a linear fit to the 72.009 subharmonic data. The data shown here was collected 7/15/10 for a full accumulation time of 925 μs and 400 μs added store time.

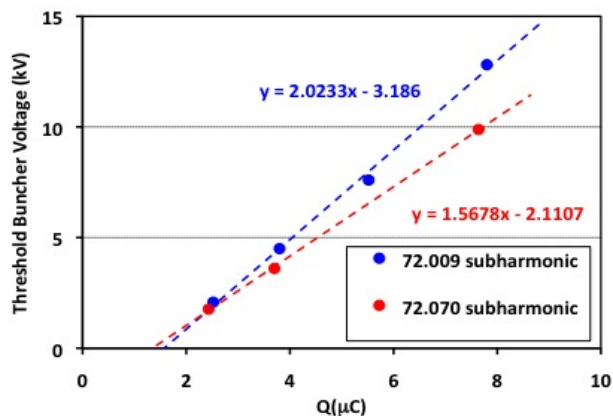


Figure 7: Comparison of instability threshold curves for ring operation at the 72.009 (blue curve) and 72.070 subharmonic (red curve) of the linac bunch frequency. Data plotted here was collected 7/15/10 for a PW = 290 ns, 925 μs accumulation and 400 μs store time after end of accumulation.

During the investigation we did not have enough beam time to take 3 or 4-point threshold curves for every PW. Instead, we took standard threshold curves (where intensity is varied with all other parameters fixed) for the largest PW=290 ns (Figure 7) and collected instability threshold voltage data as a function of PW for the full accumulation and store times (Figure 6). The data of Figure 6 confirm that the short pulse instability still exists for the 72.070 subharmonic frequency and also shows that the behavior at the 72.009 subharmonic frequency is similar to the experience of previous years for 72.000 subharmonic frequency. A more detailed discussion and comparison of the two operating frequencies follows in the next section.

The data in Figure 7 are similar to and consistent with measurements in 2006 where the 72.070 subharmonic frequency systematically lowered the instability threshold voltage. The latter was one reason for adopting the 72.070 subharmonic frequency for routine production beam, i.e., PW = 290 ns. Additional reasons included a reduction in high frequency structure on the longitudinal beam pulse and beam position monitors (BPM) plus a reduction in electron cloud generation in drift spaces.

WHAT IS DIFFERENT NOW?

The search for a beam dynamics explanation of the surprising difference in instability thresholds as a function of PW for the integer and non-integer subharmonic ring frequencies motivates a more detailed comparison of the two setups. The main difference is in the filling of longitudinal phase space as depicted schematically in Figure 8 for the integer subharmonic (72.000) and a non-integer subharmonic (72.100). For the integer subharmonic ring frequency, the micropulses with the linac rf structure are injected on top of the micropulses of previous turns while, for the non-integer subharmonic, the micropulses have a slight delay on each successive turn and fill in the space between microbunches.

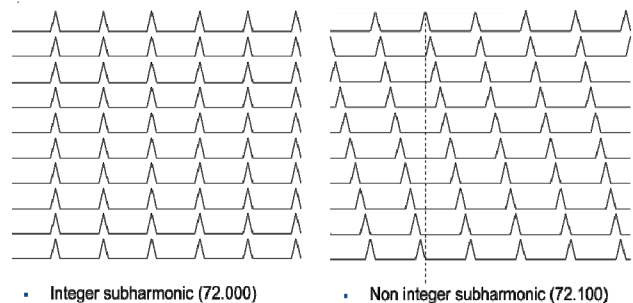


Figure 8: Schematic representation of turn-by-turn injection of micropulses (beam bunches with the time structure of the linac rf, 201.25 MHz) into the ring. The abscissa is the PSR rf phase and sequential turns (micropulses which are about 58 micropulses for a PW=290) are shown on the ordinate. Integer subharmonic (72.000) injection is shown on the left and non-integer subharmonic (72.100) on the right.

This “stacking” or “pileup” of micropulses results in large space charge forces at the micropulse locations and very few particles (and little space charge) between them. This effect is shown in the longitudinal phase space distribution of Figure 9 obtained from an ORBIT [4] simulation of production beam accumulation in PSR at the integer subharmonic. The projection of the longitudinal phase space distribution of Figure 9 onto the phase axis is plotted in Figure 10 and shows significant high frequency structure that is also observed experimentally.

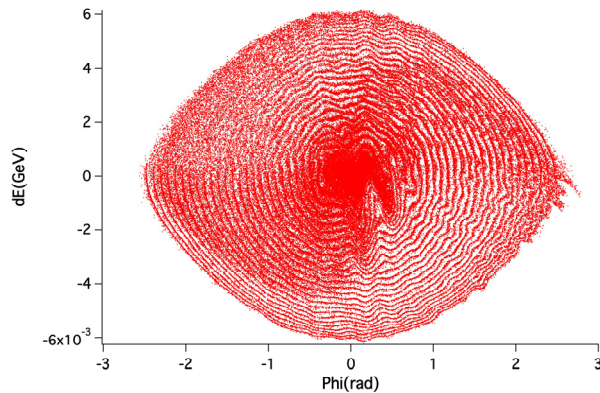


Figure 9: Longitudinal phase space distribution (dE vs. the phase, Phi) obtain from an ORBIT simulation of beam accumulation (625 μ s, for 5.2 μ C of stored charge) with the integer subharmonic rf (10kV). Energy loss from stored beam particles that traverse the stripper foil (400 microgram/cm²) is included as is transverse and longitudinal space charge plus the complex impedance of the heated inductive inserts in the ring [5, 6].

For the non-integer subharmonic regime depicted in the right hand graphic of Figure 8, the micropulses on subsequent turns are injected with a slight phase or time shift with respect to the micropulse of the previous turn. This fills the space between micropulses in 10 turns for the 72.100 or 14 turns for the 72.070 subharmonic. The chopping for minipulses is synchronized to the ring frequency such that the pattern repeats every 10 turns for 72.100 or 14 turns for 72.070. This “micropulse painting” leads to a much smoother distribution in longitudinal phase space (no ridge and valley structure) and significantly reduced high frequency structure on the longitudinal bunch profile.

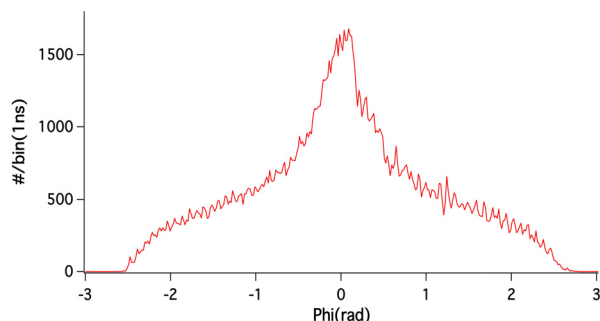


Figure 10: Histogram of the projection of the phase space distribution of Figure 9 onto the phase axis.

A reasonably good approximation to the longitudinal phase distribution obtained with the 72.070 subharmonic ring rf “micropulse painting” can be obtained from an ORBIT simulation with no linac rf bunch structure on the injected beam. Results from such a simulation for accumulation of 5.2 μ C of stored charge in 625 μ s are plotted in Figure 11. Included in the simulation are energy losses in the stripper foil (400 microgram/cm²), transverse and longitudinal space charge plus the complex impedance of the heated inductive inserts in the ring.

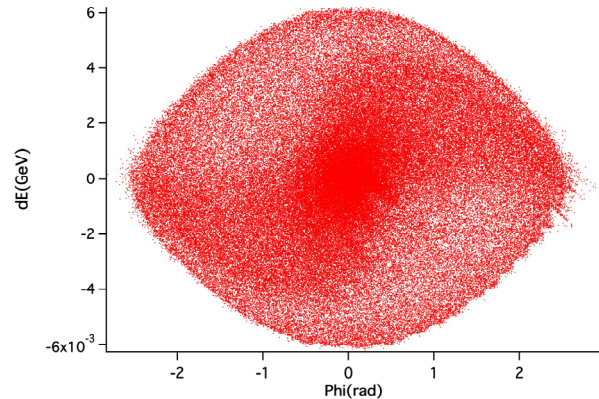


Figure 11: Longitudinal phase space distribution from an ORBIT simulation with no linac 201.25 MHz bunch structure on the injected beam.

A comparison of wall current monitor signals for the two ring frequencies is shown in Figure 12 and reveals the reduced high frequency structure for the non-integer 72.070 subharmonic. Digital fft analysis of the last 20 μ s (55 turns) of the wall current signals showed that the frequency spectra (mostly revolution harmonics) in the range 75-225 MHz (revolution harmonics 28-80) were down 12-15 db for the non-integer subharmonic (72.070) compared to the integer subharmonic (72.000).

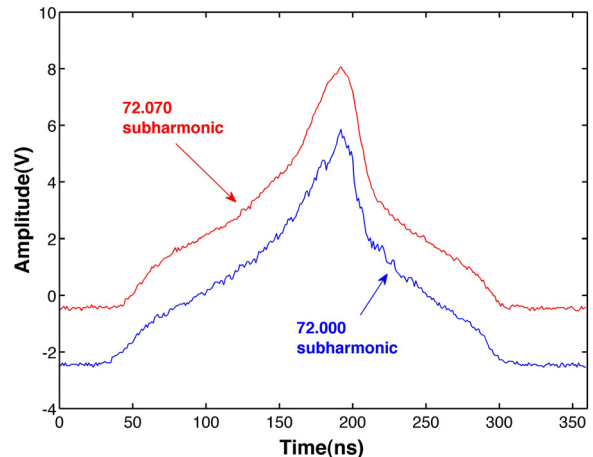


Figure 12: Wall current monitor signals at the last turn in PSR just before extraction for integer subharmonic (72.000) and non-integer subharmonic (72.070) ring frequencies. Data collected 7/15/2006 for 825 μ s of accumulation and 200 μ s of added store time.

Other benefits of the non-integer (72.070) subharmonic operation include reduced noise in the ring BPMs,

somewhat lower instability threshold curves (e.g., Figure 7) and reduced electron cloud signals in drift spaces (see Figure 13). The electron cloud signal for integer subharmonic (blue trace) in Figure 13 is a factor of 5-10 larger than for the non-integer case (red trace) and shows much greater short-term (tens of turns) fluctuations before the end of accumulation.

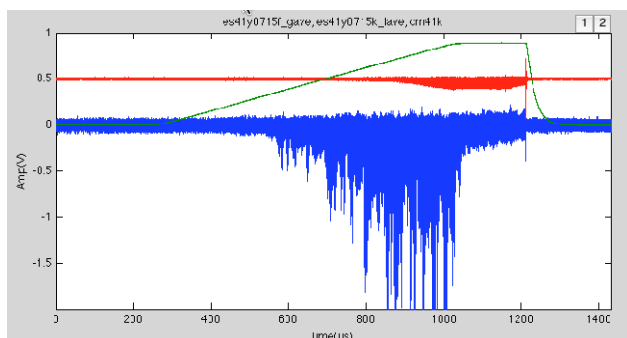


Figure 13: Comparison of electron signals from a drift space diagnostic for integer subharmonic (72.000, blue trace) and non-integer subharmonic (72.070, red trace). They are also compared with the stored current beam current signal (green trace, arbitrary units). The red trace has been displaced 0.5 V in the vertical for clarity. Data shown here were collected 7/15/2006 for 825 μ s of accumulation and 200 μ s of added store time.

The data, simulations and analysis in this section have provided a more detailed comparison of the beam characteristics for the two ring frequencies but have not established a clear beam dynamics explanation for the large difference in behavior of the instability thresholds as function of PW. The short pulse instability behavior for the non-integer subharmonic is reasonably consistent with the instability model of Blaskiewicz et al [3]. In this model the rf voltage at threshold is proportional to $(PW)^{-3}$, which approximately fits the red (72.070 subharmonic) curve in Figure 6 or the slopes of the instability thresholds of Figures 2 and 3 as shown in Figure 5.

CONCLUSIONS

In 2009 the “short pulse instability” phenomenon was discovered at PSR for the non-integer subharmonic (72.070) ring frequency. It was a surprise because the instability threshold buncher voltage as a function PW was quite different for the integer subharmonic (72.000) frequency in use until 2007. As it turns out, the threshold

voltage as a function PW for the non-integer subharmonic frequency is reasonably consistent with the Blaskiewicz model [3]. Thus, the real beam dynamics question is why the integer subharmonic ring frequency leads to more stable short pulses, where the threshold voltage is proportional to PW. Perhaps the answer lies with the space charge effects of the strong ridge and valley structure of the longitudinal phase space distribution or the increased high frequency longitudinal structure for the integer subharmonic (72.000) operating regime. A theoretical investigation along these lines would be valuable.

ACKNOWLEDGMENTS

We gratefully acknowledge the excellent support provided by the AOT division at LANL. The expertise and enthusiastic response of the accelerator operators was of immense value during the execution of our beam experiments. One of us (R. Macek) would also like to acknowledge useful discussion with M. Blaskiewicz, M. Plum, and P. Channell.

REFERENCES

- [1] D. Neuffer et al, “Observations of a fast transverse instability in the PSR”, NIM **A321**, p. 1(1992).
- [2] R. Macek, Series of lectures on electron cloud effects at PSR given at the Electron Cloud Feedback Workshop, Indiana University, Bloomington, IN, March 15-18, 2004. website: <http://physics.indiana.edu/~shylee/ap/mwpc/epfeedback.html>.
- [3] M. Blaskiewicz et al, “Electron cloud instabilities in the Proton Storage Ring and Spallation Neutron Source”, PRST-AB **6**, 014203 (2003).
- [4] J. A. Holmes et al, “ORBIT: Beam Dynamics Calculations for High Intensity Rings”, ICFA Beam Dynamics Newsletter **30**, April 2003.
- [5] M. Plum et al, “Experimental study of passive compensation of space charge at the Los Alamos National Laboratory Proton Storage Ring”, PRST-AB **2**, 064201(1999).
- [6] C. Beltran et al, “Calculations and observations of the longitudinal instability caused by the ferrite inductors at the Los Alamos Proton Storage Ring (PSR)”, Proceedings of PAC 2003, paper TOPD004, p 326 (2003).